Cervical Epithelial Cells

Subjects: Oncology | Obstetrics & Gynaecology | Pathology

Contributor: Katarzyna Sitarz, Krzysztof Czamara, Slawa Szostek, Agnieszka Kaczor

Using Raman microscopy, we investigated epithelial cervical cells collected from 96 women with squamous cell carcinoma (SCC) or belonging to groups I, IIa, IIID-1 and IIID-2 according to Munich III classification (IIID-1 and IIID-2 corresponding to Bethesda LSIL and HSIL groups, respectively). All women were tested for human papillomavirus (HPV) infection using PCR. Subcellular resolution of Raman microscopy enabled to understand phenotypic differences in a heterogeneous population of cervical cells in the following groups: I/HPV−, IIa/HPV−, IIa/HPV−, LSIL/HPV−, LSIL/HPV+, HSIL/HPV−, HSIL/HPV+ and cancer cells (SCC/HPV+). We showed for the first time that the glycogen content in the cytoplasm decreased with the nucleus size of cervical cells in all studied groups apart from the cancer group. For the subpopulation of large-nucleus cells HPV infection resulted in considerable glycogen depletion compared to HPV negative cells in IIa, LSIL (for both statistical significance, ca. 45%) and HSIL (trend, 37%) groups. We hypothesize that accelerated glycogenolysis in large-nucleus cells may be associated with the increased protein metabolism for HPV positive cells. Our work underlines unique capabilities of Raman microscopy in single cell studies and demonstrate potential of Raman-based methods in HPV diagnostics.

Keywords: human papillomavirus ; glycogen ; cervical cancer ; cervical dysplasia ; Raman microscopy ; glycogenolysis

1. Subcellular Distribution of Glycogen in Cervical Epithelial Cells

Raman imaging was used to analyze human epithelial cervical cells obtained from 96 patients classified to eight groups according to Munich III system [1] and HPV tests: I/HPV$^-$, IIa/HPV$^-$, IIa/HPV$^+$, LSIL/HPV$^-$, LSIL/HPV$^+$, HSIL/HPV$^-$, HSIL/HPV$^+$ and cancer cells – squamous cell carcinoma (SCC/HPV$^+$; for number of patients see Table S1). The cluster analysis (CA, a statistical method enabling to classify spectra according to a chemical composition) was used to determine distribution of main subcellular structures. As the representative microphotographs (Figure 1A,C) and, in particular CA images (Figure 1B,D) show, the size of cell nuclei in epithelial cells varies significantly spanning the range of 4.5–15.8 µm (the class denoted in blue in Figure 1B,D, the marker Raman band due to the symmetric phosphodiester stretching vibration at 785 cm^{-1}, Figure 1E).

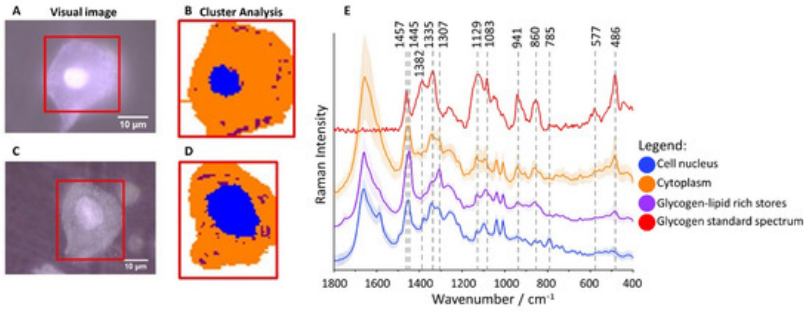

Figure 1. Glycogen-rich cytoplasm and stores in cervical epithelial cells. Microphotographs of representative cells ((**A**): IIa/HPV$^-$; (**C**): IIa/HPV$^+$) with a cell nucleus of diameter smaller and bigger than 10 µm, respectively, and CA images (**B**,**D**) showing distribution of cell nuclei (blue class) and glycogen/lipid-rich stores (maroon class) in the cytoplasm (orange class). The average Raman spectra of cell nuclei, cytoplasm and glycogen/lipid stores (**E**) averaged over all measured cells from all groups (in total 560 cells) along with the spectrum of the glycogen standard.

Cytoplasm (denoted in orange) is rich in glycogen (Figure 1B,D) as the averaged spectrum clearly demonstrates due to presence of characteristic marker bands at 486, 577, 860, 941, 1083, 1129, 1335 and 1382 cm^{-1} (Figure 1E). Additionally, structures of changeable size and number spread in whole cytoplasm containing lipids (exhibiting characteristic bands due to lipids at 1307 and 1445 cm^{-1}) and glycogen can be separated (denoted in maroon, Figure 1B,D). Glycogen plays an important role in early metastasis [2], fuels glycolysis in cancer cells [2] and it is known that its content decreases due to

carcinogenesis [3]. Therefore, based on Raman microscopy and statistical methods, we evaluated the glycogen level in epithelial cells in all studied groups to determine how it is related to the nucleus size, cervical precancerous changes, and HPV infection.

2. Glycogen Content Decreases with the Increase of Nuclei Size of Cervical Epithelial Cells in I, IIa, LSIL and HSIL Groups, but Not the Cancer Group

In neoplastic cells, the diameter of nuclei is bigger than in healthy cells [4]. This phenomenon is used in pathomorphology to assess pathological changes in cells, including cervical cancer [4]. Subcellular resolution of Raman microscopy and the chemical characteristics of cell components enabled to separate cells differing by the size of nuclei. The chemical composition of nuclei for cells with nuclei of large and small diameter (defined arbitrarily as d ≥ 10 µm and < 10 µm, respectively) is, however, uniform independently on the group considered (Figure S1). It is in line with the finding that regardless of its size, the amount of chromatin in the nuclei of cervical epithelial cells is similar [5].

Nevertheless, the glycogen content (evaluated as the integral intensity of the characteristic band at 486 cm^{-1} both due to glycogen dispersed in the cytoplasm and glycogen in the form of glycogen-lipid-rich stores) occurs to be significantly decreased in cells with large cell nuclei in I/HPV$^-$, IIa/HPV$^+$ and LSIL/HPV$^+$ (Figure 2). Additionally, in groups IIa/HPV$^-$ and both HSIL groups there is a clear tendency to a reduced amount of glycogen in cells with large nuclei, although this relationship is not statistically significant, for HSIL groups quite obviously due to limited number of cells with the large cell nuclei. For the cancer groups the glycogen content is not related with the size of the nucleus.

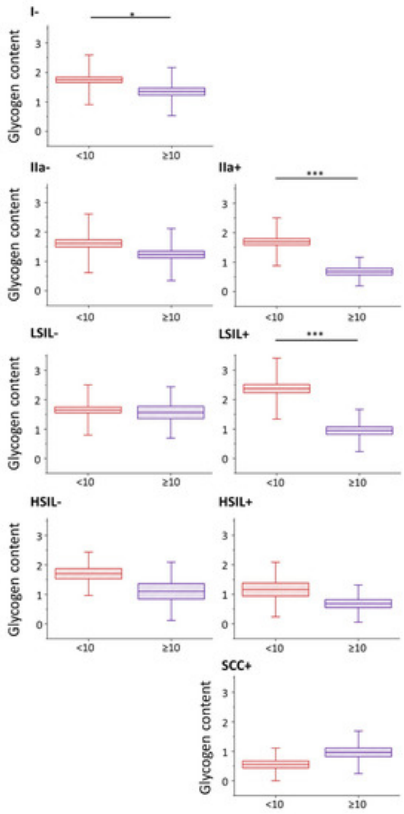

Figure 2. Glycogen content in epithelial cervical cells depending on the nucleus size. The analysis of the glycogen content in the cytoplasm of cervical epithelial cells with cell nuclei of a diameter <10 µm (burgundy color) and ≥10 µm (violet color) based on the integral intensity of the glycogen marker band at 486 cm^{-1}. Graphs present individual groups of cells: I/HPV$^-$, IIa/HPV$^-$, IIa/HPV$^+$, LSIL/HPV$^-$, LSIL/HPV$^+$, HSIL/HPV$^-$, HSIL/HPV$^+$ and SCC/HPV$^+$. Mean values ± SEM are given as box plots: mean (horizontal line), SEM (box), SD (whiskers). * $p < 0.05$, *** $p < 0.001$.

A decreased level of glycogen in cervical cells is usually attributed to increased glycogenolysis [6]. Our results show that for cervical cells, particularly with cell nuclei of large diameter, show glycogen depletion that may be related with accelerated glycogenolysis. Moreover, the presence of HPV infection additionally influences the glycogen metabolism as the differences between the glycogen levels in cells with large and small-diameter cell nuclei are bigger in HPV$^+$ groups compared to HPV$^-$ (the decrease in the glycogen level for cells with nuclei d ≥ 10 compared to d < 10 µm equals for IIa/HPV$^-$ vs. IIa/HPV$^+$: 24% vs. 60%; LSIL/HPV$^-$ vs. LSIL/HPV$^+$: 5% vs. 60% and HSIL/HPV$^-$ vs. HSIL/HPV$^+$: 35% vs. 41%).

Patients classified as group IIa usually present as both cytologically and histologically negative. Interestingly, the presence of large-diameter nucleus cells of modified glycogen metabolism in the IIa/HPV$^+$ group suggests that pathological changes already may occur in cells in this group, which until now were considered dysplasia-free, although this hypothesis undoubtedly requires further studies. To investigate in more detail how a glycogen level is influenced by the dysplasia progress and HPV presence, the statistical analysis of the cytoplasm glycogen content in cells from all groups was performed without separation for cells according to the nucleus size (Figure S2 and S3). Interestingly, our results show that if the large-diameter (that are less numerous in population of a given group) cell nuclei are not excluded, the cells in various groups behave as previously reported, i.e., the glycogen content is decreased in cancer cells [6][7] and increased glycogen metabolism in HPV$^+$ vs. HPV$^-$ cells cannot be observed. It underlines importance of the single cells approach and subcellular resolution of Raman microscopy used in this work.

3. HPV Accelerates Glycogen Metabolism in Cervical Epithelial Cells

The results of the statistical analysis of the glycogen level (Kruskal–Wallis test, U'Mann–Whitney test) in all studied cells are presented in Figure 3 (also in Table S2).

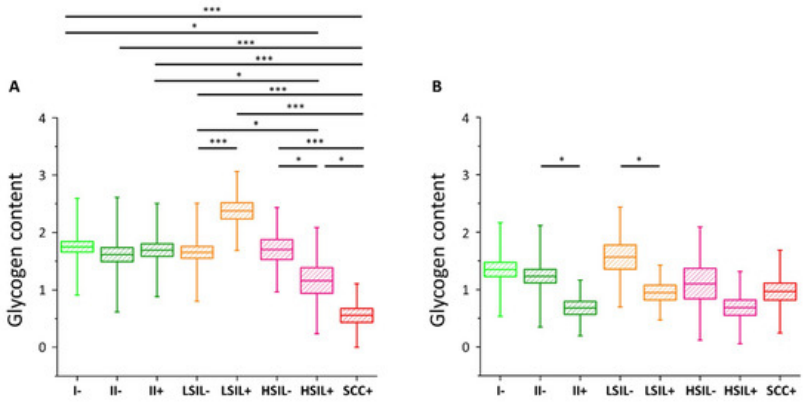

Figure 3. Glycogen content in the cytoplasm of cervical epithelial cells depending on HPV presence**.** The comparison of the glycogen content in the cytoplasm of cervical epithelial cells in studied groups: I/HPV$^-$ (bright green), IIa/HPV$^-$ (dark green), IIa/HPV$^+$ (dark green), LSIL/HPV$^-$ (orange), LSIL/HPV$^+$ (orange), HSIL/HPV$^-$ (pink), HSIL/HPV$^+$ (pink), SCC/HPV$^+$ (red) obtained by calculations of the integral intensity of the band at 486 cm^{-1} for cells with the nuclei of a diameter <10 µm (**A**) and ≥10 µm (**B**). Mean values ± SEM are given as box plots: mean (horizontal line), SEM (box), SD (whiskers). * $p < 0.05$, *** $p < 0.001$ (only key significances, described in the text, were presented).

As we have clearly identified small-diameter nuclei cells as metabolically different that the large-diameter nuclei cells, we compared separately these two groups of cells. For cells with small nuclei (Figure 3A) for I/HPV$^-$, IIa/HPV$^-$, IIa/HPV$^+$, LSIL/HPV$^-$, and HSIL/HPV$^-$ there are no statistically significant differences between the level of glycogen in the cytoplasm. The LSIL/HPV$^+$ shows a difficult to rationalize increase in the glycogen level. Contrarily, the cells of patients with the cervical cancer have accelerated glycogen metabolism compared to all the above-mentioned groups, what agrees with previous findings showing that glycogenolysis is increased in cancer cells [6]. This effect is also observed by us for the for HSIL/HPV$^+$ group confirming their phenotypic similarity to SCC/HPV$^+$ cells.

In the case of cells possessing large-diameter cell nuclei (Figure 3B) the results are strikingly different. The level of glycogen in the cytoplasm of large-nucleus cells in HPV$^-$ groups I, IIa, LSIL and HSIL is similar. However, the results clearly show a decrease of the glycogen content for cells infected with HPV that is statistically significant for IIa and LSIL groups and shows a trend for the HSIL group. Reduction in the glycogen level equals to 45% for IIa/HPV$^+$ vs. IIa/HPV$^-$, 46% for LSIL/HPV$^+$ vs. LSIL/HPV$^-$ and 37% for HSIL HPV$^+$ vs. HSIL/HPV$^-$, respectively. Moreover, these changes of the glycogen content are not dependent on age (Figure S4).

For the SCC/HPV$^+$ group the average glycogen content does not significantly differ from most of the groups (Figure 3B). In combination with the data in Figure 3A, showing the lowest glycogen level for the SCC/HPV$^+$ group, these results underline the importance of separate analysis of the cells with large and small cell nuclei. The key observation of this study is a very significant glycogen depletion in these large-nucleus cells in HPV$^+$ groups compared with the respective HPV$^-$ groups (results summarized in Figure 4).

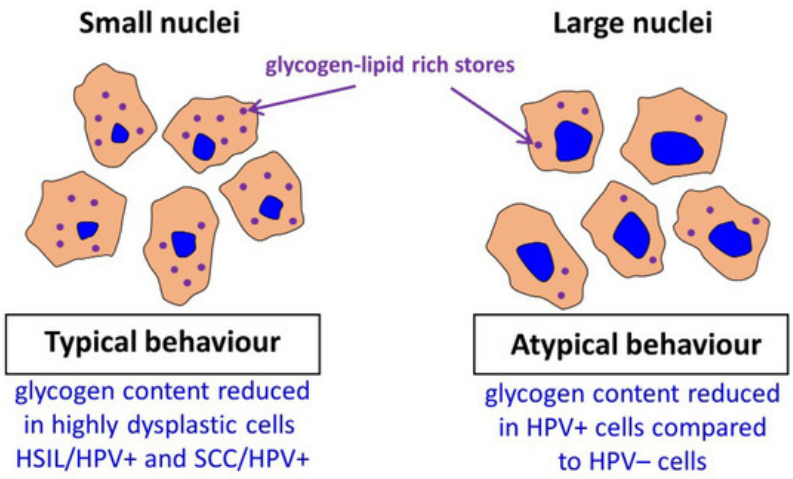

Figure 4. Summary of obtained key results.

Previously Curtis et al. [2] reported a considerable decrease in the glycogen level (the mobilization of glycogen stores) in late metastatic cells compared to early ones. The additional energy obtained in cancer cells is necessary to begin high-energy tasks such as migration, invasion, and further metastasis. It is hypothesized that the process of glycogen mobilization and possible increased glycolysis is used by large-nucleus HPV^+ cells for increased protein synthesis [8]. We also conclude that the factors causing expanding of a cell nucleus considerably change also cellular carbohydrate metabolism and that it may be related with neoplastic transformation. This interesting phenomenological observation has to be studied in the future to understand a genetic background of this phenomenon. To confirm results obtained by Raman microscopy, the gold standard, i.e., PAS staining of the cells was performed (Figure 5).

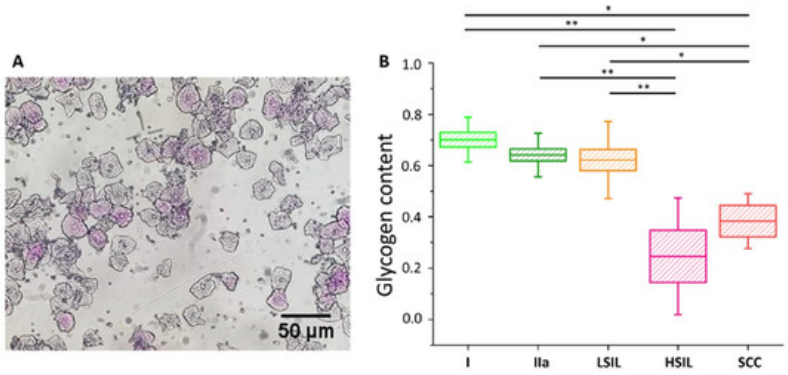

Figure 5. Glycogen content in the cytoplasm of cervical epithelial cells evaluated using a PAS staining method**.** An illustrative photograph of a sample of cervical epithelial cells stained by PAS (**A**). The analysis of the glycogen content (**B**) in the cytoplasm of cervical epithelial cells according to the division of patients into groups I (bright green), IIa (dark green), LSIL (orange), HSIL (pink) and SCC (red). Glycogen content was determined by optical evaluation in a light microscope after PAS staining by calculations of the average percentage of stained cells among all cells stained in individual groups. Each point on the graph corresponds to the average result for one patient (B). Values were given as mean ± SEM and were shown in box plots: mean (horizontal line), SEM (box), minimal and maximal values (whiskers). * $p < 0.05$, ** $p < 0.01$.

The cells were divided into five groups, i.e., I, IIa, LSIL, HSIL and SCC (for number of patients see Table S3). The additional separation due to the diameter of the cell nucleus was not possible due to the characteristics of PAS method (nuclear diameters could not be exactly determined). As Figure 5 shows, the average percentage of cells that were successfully stained with PAS is similar in groups I, IIa and LSIL, but significantly decreases with the progression of pathological changes, i.e., for HSIL and SCC groups. The results of PAS staining confirm the findings of spectroscopic measurements (Figure S3 for direct comparison) validating the proposed Raman-based approach.

Our results show that a Raman-based methodology may be potentially used for fast HPV testing due to the decreased level of glycogen in the cytoplasm in HPV^+ cells compared to HPV^- cells for a given group. Therefore, to preliminary evaluate possibilities of the Raman-based approach, the fiber probe Raman setup, applicable for application in healthcare facilities, was used to measure in a fast manner the glycogen content in a pellet of cervical cells showing that good quality Raman spectra of cervical cells can be obtained (Figure S5). Further large data study is necessary to confirm if infection of HPV is detectable using such an approach.

4. Conclusions

In this study, we assessed differences in the cytoplasm glycogen level of cervical epithelial cells, collected from 96 women, depending on the presence of HPV infection, dysplastic changes and nucleus diameter using Raman microscopy and chemometric data analysis. The applied methodology appeared to be crucial to account for a considerable heterogeneity of cells in studied groups (I/HPV$^-$, IIa/HPV$^-$, IIa/HPV$^+$, LSIL/HPV$^-$, LSIL/HPV$^+$, HSIL/HPV$^-$, HSIL/HPV$^+$ and SCC/HPV$^+$). In particular, due to the subcellular resolution of Raman imaging, we were able to separate a subgroup of cervical cells with large (over 10 µm) diameter of nuclei, showing unexpected chemical and metabolic characteristics.

As our results demonstrate, in cervical cells glycogen is both dissolved in cytoplasm and aggregated with lipids in the form of glycogen-lipid-rich granules. For cells with small-diameter nuclei, the global level of glycogen in the cytoplasm is similar for considered groups apart from the SCC/HPV$^+$ group that is characterized by a decrease in the glycogen content in agreement with previous studies [6] and HSIL/HPV$^+$ group that is phenotypically similar to SCC/HPV$^+$. Additionally, somewhat difficult to rationalize is an increase in the LSIL/HPV$^+$ level. Importantly, there are no differences between the glycogen content for small-diameter cells in the HPV$^+$ and HPV$^-$ respective groups. Contrarily, for the subpopulation of large-nucleus cells, the cytoplasm glycogen level is significantly reduced of about 37–46% for HPV$^+$ cells compared to HPV$^-$ cells. It shows that for this subpopulation of cells, glycogen metabolism accelerates with HPV infection. The considerable depletion of the glycogen level in HPV infected cells may be associated with molecular pathways related with HPV E6 and E7 proteins [9][10] and increased energetic needs in the HPV infected cells for protein synthesis and virus replication. The mobilization of glycogen stores, i.e., increased glycogenolysis in late compared to early metastatic cells was previously attributed in ovarian cancer cells to their increased capabilities for migration and invasion [11]. Understanding of molecular basis of accelerated glycogenolysis in HPV infected cervical cells requires further research to shed light on mechanism of HPV-induced carcinogenic transformation.

Last, but not least, lack of reagents and speed of Raman spectroscopy could be advantageous in HPV diagnostics compared to the DNA-HPV method. Raman spectroscopy may be in future a base for a simple, automatized test for HPV; however, it certainly requires further testing on a bigger cohort of patients and improvement of the methodology.

References

1. Cirkel, C.; Barop, C.; Beyer, D.A; Method comparison between Munich II and III nomenclature for Pap smear samples. *Geburtshilfe und Frauenheilkunde* **2015**, *16*, 203–207, .
2. Curtis, M.; Kenny, H.A.; Ashcroft, B.; Salomon, A.R.; Nebreda, A.R.; Lengyel, E; Fibroblasts Mobilize Tumor Cell Glycog en to Promote Proliferation and Metastasis. *Cell Metab.* **2019**, *29*, 141–155.e9, 10.3410/f.733939084.793550365.
3. Hervieu, A.; Kermorgant, S; The Role of PI3K in Met Driven Cancer: A Recap. *Front. Mol. Biosci.* **2018**, *5*, 86, 10.3389/f molb.2018.00086.
4. Zink, D.; Fischer, A.H.; Nickerson, J.A; Nuclear structure in cancer cells. *Nat. Rev. Cancer* **2004**, *4*, 677–687, .
5. Sørensen, F.B.; Bichel, P.; Jakobsen, A; DNA level and stereologic estimates of nuclear volume in squamous cell carcin omas of the uterine cervix. A comparative study with analysis of prognostic impact. *Cancer* **1992**, *69*, 187–199, .
6. Warburg, O; On the origin of cancer cells. *Science* **1956**, *123*, 309–314, .
7. Christos Zois; Adrian L. Harris; Glycogen metabolism has a key role in the cancer microenvironment and provides new targets for cancer therapy. *Journal of Molecular Medicine* **2016**, *94*, 137-54, 10.1007/s00109-015-1377-9.
8. Sonia C Dolfi; Leo Li-Ying Chan; Jean Qiu; Philip M Tedeschi; Joseph Bertino; Kim M. Hirshfield; Z. N. Oltvai; A Vazque z; The metabolic demands of cancer cells are coupled to their size and protein synthesis rates. *Cancer & Metabolism* **2 013**, *1*, 20, 10.1186/2049-3002-1-20.
9. Mary C. Thomas; Cheng-Ming Chiang; E6 Oncoprotein Represses p53-Dependent Gene Activation via Inhibition of Pro tein Acetylation Independently of Inducing p53 Degradation. *Molecular Cell* **2005**, *17*, 251-264, 10.1016/j.molcel.2004.1 2.016.
10. Daeyoup Lee; Chunghun Lim; Taegun Seo; Hyockman Kwon; Hyesun Min; J Choe; The Viral Oncogene Human Papillo mavirus E7 Deregulates Transcriptional Silencing by Brm-related Gene 1 via Molecular Interactions. *Journal of Biologic al Chemistry* **2002**, *277*, 48842-48848, 10.1074/jbc.m203583200.
11. Rodríguez-García, A.; Samsó, P.; Fontova, P.; Simon-Molas, H.; Manzano, A.; Castano, E.; Rosa, J.L.; Martinez-Outsh oorn, U.; Ventura, F.; Navarro-Sabate, A.; et al. TGF-β1 targets Smad, p38 MAPK, and PI3K/Akt signaling pathways to i nduce PFKFB3 gene expression and glycolysis in glioblastoma cells. FEBS J. 2017, 284, 3437–3454.